LOG -VANE SCOUR IN CLEAR WATER CONDITION

S. Pagliara[a*], L. S. Hassanabadi[a] and S. M. Kurdistani[a]
[a] *Department of Energy, Systems, Land and Structures Engineering , University of Pisa*

ABSTRACT: Log-Vane is a grade-control structure of common use to stabilize riverbed and river banks. The purpose of this paper is to study the scour phenomena downstream of Log-Vanes in straight rivers. The main goal is to obtain design equations to determine the main scour parameters and the scour morphology. All the experiments have been carried out in a horizontal channel and in clear water conditions. Log-Vanes made of wood, with different heights and vane angles were tested. Different hydraulic conditions including densimetric Froude numbers, water drops and tail water values were tested. Results show that the tail water depth is an important variable to determine the maximum scour depth. The vane angle results to be an important parameter to predict the scour parameters. Dimensional analysis allows to derive design equations useful to estimate the maximum scour depth, maximum length of the scour and maximum height and length of the dune.

KEYWORDS: Log-Vane; Hydraulic Structures; River Restoration; River Grade-Control; Scour

[*] Correspondence to: S. Pagliara, Prof., Department of Energy, Systems, Land and Structures Engineering , University of Pisa, 22, Via Gabba, 56122, Pisa, Italy, +390502217717. E-mail: s.pagliara@ing.unipi.it

INTRODUCTION

River restoration including river grade control, bank protection, water quality and aquatic habitat is an important aspect of river engineering. Log-Vanes, as single-arm structures, are placed in the riverbed and are usually submerged even during low flows. In the presence of Log-Vanes, secondary flow leads to scour pools. Jansen et al. 1979, Odgaard and Spoljaric 1986, Odgaard and Mosconi 1987 and Odgaard and Wang 1991 gave major contributions on submerged vanes hydraulic. In the scientific literature there are no comprehensive studies on scour downstream of Log-Vane structures. The classical literature includes important researches on local scour like Schoklitsch (1932), Veronese (1937), Hassan and Narayanan (1985), Farhoudi and Smith (1985), Mason and Arumugan (1985), Bormann and Julien (1991), Whittaker and Jaggi (1996), Robinson et al. (1998) and Dey and Sarkar (2006a and b, 2008).

Few contributions are focused on scour downstream of grade-control structures. Shields et al. (1995) arranging a field measurement study in north-west Mississippi, discovered the effects of stone grade-control structures on fish migration. Rosgen (2001) presented design details of a series of in-stream structures including Log-Vane. Structures such as Log-Vane, J-Hook Vane block ramps and Rock-Vanes are open hydraulic structures with no obstruction for fish migration and are known as eco-friendly structures. Pagliara (2007) obtained simple expressions to determine the scour depth and length downstream of block ramps carrying out a series of tests in clear water condition. The scour morphology was further explained by Pagliara and Palermo (2008). Pagliara et al. 2012 described localized scour phenomena downstream of block ramps for live-bed. Bhuiyan et al. (2007) compared the scour development downstream of W-weirs with the previous study's results. Scurlock et al. (2011, 2012a and b) conducted experimental study on three types of in-stream structures. Pagliara and Kurdistani (2013) and Pagliara et al. (2013) analyzed the scour geometry in straight rivers downstream of Cross-Vane and J-Hook vane structures respectively. Recently Pagliara et al. (2014) studied scour morphology downstream of rock W-weir in clear water condition. The main purpose of this study is to experimentally analyze the scour geometry and pattern downstream of Log-Vane structures in horizontal straight channels.

EXPERIMENTAL SETUP

All the experiments have been carried out in a horizontal channel 0.8 m wide, 20 m long and 0.75 m deep located in the PITLAB hydraulic laboratory of the University of Pisa. Stable inflow was supplied by an overhead tank. The flow discharge was measured using a calibrated tank with a precision of ±0.1 l/s. An ultrasonic distance meter "Baumer" sensor with precision of 0.001 m has been used to read the water surface profile and the bathymetry of the mobile bed. Fig.1 shows a plan, a stream wise view A-A and a cross section D-D of the channel; detail C shows that each structure was made with three pieces of wood. Two stones are attached to each structure to keep it stable on the channel bed. In Fig. 1, α is the vane angle in respect to the river bank, l is the length and h_{st} is the height of the structure. Table 1 shows the characteristics of the studied Log-Vanes.

In Fig. 1, Δy is the difference between the water surface upstream and downstream of the structure, B is the channel width, z_m is the maximum scour depth, l_m is the length of the scour, z'_m is the maximum height of the ridge, l'_m is the ridge length and ξ is the minimum distance of the scour hole from the channel bank. All the tests data are shown in Table 2.

The densimetric particle Froude number is defined as $F_d = Q'/(l.\ h_{st}.[g.(G_s - 1).d_{50}]^{0.5})$, where $Q'=(b/B)Q$ is the effective flow discharge, $G_s = \rho_s/\rho$, in which ρ_s is the bed material density and ρ the water density, d_{50} is the mean particle diameter and g the gravitational acceleration. Uniform non-cohesive sand with a $\sigma = (d_{84}/d_{16})^{1/2}$=1.16, G_s = 2.60 and d_{50} = 1.70 mm was used. At the beginning of each experiment, the channel bed was carefully leveled. All the tests have been conducted in clear water condition.

Three series of experiments were carried out. The first series included tests on Log-Vane in a horizontal channel with $\alpha = 30°$ for different values of the height of the structure, discharge and Δy. The second and third series of experiments were done for Log-Vanes with vane angle of 60° and 90° respectively. The duration of tests was long enough in order to reach an equilibrium bed condition depending on the single test (between one to three hours). Fig. 2a depicts view from upstream during a test run and Fig. 2b shows view from downstream at the end of an experiment.

RESULTS AND DISCUSSION

Dimensional analysis has been applied to obtain analytical functions in order to predict the main scour parameters downstream of Log-Vanes such as maximum scour depth, maximum scour length, maximum height and length of the ridge and minimum distance of the scour hole from the canal bank. For the maximum scour depth the main variables are:

$$f(z_m, l, h_{st}, h_{tw}, B, \Delta y, Q, \rho_s, \rho, g, d_{50}, \alpha) = 0 \quad (1)$$

where f is functional symbol.

Based on incomplete self-similarity (Barenblatt 1987) and considering $\sin\alpha = b/l$, eq. (1) can be expressed in a power-law expression as follows:

$$z_m / h_{st} = a \cdot f'(\sin\alpha)^c\, (h_{tw}/h_{st})^e \cdot \Phi(F_d, \Delta y / h_{st}) \quad (2)$$

Where f' and Φ are functional symbols and a, c and e are constants.

Functional relation (2) can be adopted also to determine the other scour geometry parameters substituting the corresponding variable instead of z_m in the dimensional analysis process.

SCOUR MORPHOLOGY

Pagliara and Kurdistani (2013) and Pagliara et al. (2013) defined the non-dimensional scour parameter $\eta = F^2_d \cdot \Delta y/h_{st}$ and classified the scour pattern downstream of different in-stream grade-control structures. For Log-Vane in the range of $0.02 < \eta < 4$, two types of morphologies have been defined which are shown in Fig. 3. In Type A, the dune is developed beside the scour hole close to the channel bank while in Type B the dune is developed along the scour hole towards the center of the channel.

Fig. 3a depicts a scour Type B for Log-Vane with $\alpha = 90°$, $F_d = 1.92$, $\Delta y/h_{st} = 0.15$. It shows that the dune occurred in the same line as the scour hole. Fig. 3b and c show scour Type A for Log-Vane structures with $\alpha = 60°$, $F_d = 8.54$, $\Delta y/h_{st} = 0.03$ and $\alpha = 30°$, $F_d = 1.86$, $\Delta y/h_{st} = 0.09$ respectively. It is evident that both the scour and the ridge develop close to the channel bank.

Fig. 4a shows the two types of morphologies and Fig. 4b demonstrates the field of existence of each morphology type for all experimental data of Log-Vanes including all investigated angles. These experimental observations show that scour morphology is independent from Log-Vane angle. In other words for any α depending on F_d and $\Delta y/h_{st}$, morphology Type A or Type B could occur. Fig 4b shows that increasing the densimetric Froude number, the scour type changes from Type B to Type A.

SCOUR GEOMETRY

Experimental observations show the vane angle α effects in determining the different scour parameters. Therefore *l*/*B* is effective on the scour formation downstream of Log-Vanes. Based on dimensional analysis, numerical forms of eq. (2) have been obtained to predict the values of different important design scour parameters such as maximum scour depth, maximum scour length, maximum height and length of the dune and the minimum distance of the scour hole from the channel side.

Maximum Scour Depth

Tail water depth is an important parameter to predict the scour parameters. Fig. 5a shows the maximum scour depth data downstream of Log-Vane classified as a function of η , using the non-dimensional tailwater h_{tw}/h_{st} as parameter. Data are compared with J-Hook data by Pagliara et al. (2013). It indicates that the phenomenon can be expressed by eq. (3) and is independent of α.

$$z_m/h_{st}=1.6\cdot(h_{tw}/h_{st})^{-0.5}\eta^{0.3} \quad (3)$$

Fig. 5b compares the eq. (3) with the observed data of Log-Vane a $r^2 = 0.77$ is obtained and $r^2 = 0.74$ for J-Hook vane data (Pagliara et al. 2013).

Maximum Scour Length

Experimental data show that the maximum length of the scour hole varies with the vane angle α and η. Pagliara et al. (2013) presented eq. (4) to predict the maximum scour length downstream of J-Hook vanes with α = 20°. Fig.6 shows the observed non dimensional scour length data of Log-Vane structures versus η using α as parameter. Also J-Hook data are shown in Fig. 6 for comparison.

It demonstrates that for any η, by increasing the vane angle, the scour length decreases. This relationship can be expressed by eq. (5) with a correlation coefficient of 0.84. Fig. 6 shows that at low values of η (low discharges) there are similarities between Log-Vane and J-Hook scour length results but when η increases the length of the scour hole downstream of J-Hook vane becomes much larger than the one of the Log-Vane. This effect is due to the fact that, the combination of the two scour holes downstream of J-Hook leads to a unique large scour.

$$l_m/h_{st}=23.8\ \eta^{0.5} \quad (4)$$

$$l_m/h_{st}=22.9\cdot(1+(\sin\alpha)^5)^{-1.4}\eta^{0.25} \quad (5)$$

Maximum Dune Height and Length

Investigation on ridge height data shows it depends on the vane angle α and η. Pagliara et al. (2013) found eq. (6) to determine the maximum ridge height at the downstream of J-Hook vane with α = 20° which is plotted in Fig. 7a. The observed ridge height downstream of Log-Vanes versus η is shown in Fig. 7a and compared with J-Hook data. Eq. (7) with a correlation coefficient of 0.6 shows the Log-Vane data trend. It shows, for any η, that increasing the vane angle, the maximum height of the dune decreases. Fig. 7a shows that the ridge height in J-Hook vane is less than the one in Log-Vane and became very close for Log-Vane with α = 90°.

$$z'_m/h_{st}=0.6\ \eta^{0.3} \tag{6}$$
$$z'_m/h_{st}=1.3\cdot(1+(\sin\alpha)^2)^{-1}\eta^{0.35} \tag{7}$$

The experimental observations on the ridge length show that it is mainly a function of η and can be represented by a simple equation,

$$l'_m/h_{st} = 14.4\ \eta^{0.3} \tag{8}$$

Eq. (8) with data is represented in Fig. 7b together with the available J-Hook data. It shows that increasing η, the maximum length of the dune increases. It appeared that the length of the ridge downstream of J-Hook vane always is greater than the length of the ridge downstream of Log-Vane. This is a direct consequence of the scour length differences between Log-Vanes and J-Hook.
Eq. (9) found by Pagliara et al. (2013) for evaluating the ridge length downstream of J-Hook vane comparing with observed data of Log-Vane and J-Hook vane is shown in Fig. 7b.

$$l'_m/h_{st} = 31.9\ \eta^{0.6} \tag{9}$$

Distance of the Scour Hole from the Bank

Another important design parameter in scour morphology is the minimum distance of the scour hole from the canal bank. The experimental observations show that both the vane angle and the tail water depth affect this parameter. A non-dimensional parameter $X = (\xi/B)/[(\sin\alpha)\cdot(h_{tw}/h_{st})]$ is defined in which ξ is the minimum distance of the scour hole from the channel bank. The values of X versus η are shown in Fig. 8(a). Eq. (10) with $r^2 = 0.78$ express the relationship,

$$X = 0.1\ \eta^{-0.75} \tag{10}$$

or

$$\xi/B = 0.1\cdot\sin\alpha\cdot(h_{tw}/h_{st}).\eta^{-0.75} \tag{11}$$

Fig. 8(b) shows eq. (11) for different combinations of α and h_{tw}/h_{st}.

CONCLUSIONS

Buckingham theorem and incomplete self-similarity resulted in an analytical function used to predict the main scour parameters for different combinations of hydraulic conditions and Log-Vane geometries. Experimental observations showed that tail water is an important variable to predict the maximum scour depth. The vane angle plays an important role to predict the maximum scour length and the maximum height of the ridge. The results show that by increasing η, all the scour geometry parameters increase. The minimum distance of the scour hole from the channel bank depends on both the vane angle and the tail water depth. Scour typology included two types of scour. Type A where "the dune is developed beside the scour hole close to the channel bank" and Type B where "the dune is developed along the scour hole towards the center of the channel". Equations valid for the design have been established. Further studies are necessary in order to extend the parameter range and evaluate the effectiveness of the structure also in live bed conditions.

NOTATION

b	structure width
B	channel width
d_{50}	mean particle diameter
f, f'	functional symbol
F_d	densimetric Froude number = $Q'/\{l \cdot h_{st}[g(G_s-1)d_{50}]^{0.5}\}$
g	gravitational acceleration
G_s	ρ_s/ρ
h_{st}	height of the structure (average height of the stones)
l	length of the structure
l_m	scour length downstream of the structure
l'_m	ridge length
Q	flow discharge
Q'	effective flow discharge
y_0	approach flow depth
z_m	maximum scour depth downstream of the structure
z'_m	maximum ridge height
Δy	difference between water surface upstream and downstream of the structure
α	vane angle
Φ	functional symbol
η	$\mathrm{F}_d^2 \cdot \Delta y/h_{st}$
ρ	water density
ρ_s	bed material density
σ	particle uniformity factor = $(d_{84}/d_{16})^{0.5}$
ξ	minimum distance of the scour hole from the channel bank

REFERENCES

Barenblatt, G. I. 1987. Dimensional Analysis, *Gordon and Breach Science Publishers.* ISBN 3-7186-0438-8.

Bhuiyan, F., Hey, R. D. and Wormleaton, P. R. 2007. hydraulic Evaluation of W-Weir for River Restoration. *J. Hydraul. Eng., ASCE*, **133**(6): 596-609.

Bormann, N. E. and Julian, P. Y. 1991. Scour Downstream of Grade-Control Structures. *J. Hydraul. Eng. ASCE*, **117**(5): 579-594.

Dey, S., and A. Sarkar 2006a. Scour downstream of an apron due to submerged horizontal jets. *J. Hydraul. Eng. ASCE*, **132**(3), 246-257.

Dey, S., and A. Sarkar 2006b. Response of velocity and turbulence in submerged wall jets to abrupt changes from smooth to rough beds and its application to scour downstream of an apron, *J. Fluid Mech*. **556**: 387-419.

Dey, S., and A. Sarkar 2008. Characteristics of submerged jets in evolving scour hole downstream of an apron. *J. Eng. Mech*. **134** (11): 927-936.

Farhoudi, J. and Smith, K.V.H. 1985. Local scour profile downstream of hydraulic jump. *J. Hydraul. Res*., **23**(4): 343–358.

Hassan, N. M. K. N., and Narayanan, R. 1985. Local scour downstream of an apron. J. Hydraul. Eng., **111**(11): 1371–1385.

Jansen, P. Ph., Bendegom, L. van, Berg, J. van den, Vries, M. de, and Zanen, A., Eds. 1979. Principles of river engineering. *Pitman Publishing Ltd*. London, England.

Mason, P. J. and Arumugam, K. 1985. Free Jet Scour Below Dams and Flipbuckets *J. Hydraul. Eng., ASCE*, **111**(2): 220-235.

Odgard, A.J. and Mosconi, C.E. 1987. Stream bank Protection by Submerged Vanes. *J. Hydraul. Eng., ASCE*, **113**(4): 520-536.

Odgard, A.J. and Spoljaric, A. 1986. Sediment Control by Submerged Vanes. *J. Hydraul. Eng., ASCE*, **112**(12): 1164-1181.

Odgard, A.J. and Wang, Y. 1991. Sediment Management with Submerged Vanes. II: Applications. *J. Hydraul. Eng., ASCE*, **117**(3): 284-302.

Pagliara, S. 2007. Influence of Sediment Gradation on Scour Downstream of Block Ramps. *J. Hydraul. Eng., ASCE*, **133**(11): 1241-1248.

Pagliara, S., Kurdistani, S.M. 2013. Scour downstream of cross-vane structures. *Journal of Hydro-Environment Research*, 7(4): 236-242.

Pagliara, S., Kurdistani, S.M. and Santucci, I. 2013. Scour Downstream of J-Hook Vane Structures in Straight Horizontal Channels. *Acta Geophysica*, **61**(5): 1211-1228.

Pagliara, S., Kurdistani, S., and Cammarata, L. 2014. Scour of Clear Water Rock W-Weirs in Straight Rivers. *J. Hydraul. Eng., ASCE*, **140**(4), 06014002.

Pagliara, S. and Palermo, M. 2008. Scour control and surface sediment distribution downstream of block ramps. *Journal of Hydraulic Research,* **46**(3): 334–343

Pagliara, S., Palermo M., and Carnacina, I. 2012. Live-bed scour downstream of block ramps for low densimetric Froude numbers. *International Journal of Sediment Research*, **27**(3): 337–350.

Robinson, K. M., Rice, C. E., and Kadavy, K. C. 1998. Design of rock chutes. *ASAE Paper (American Society of Agricultural Engineers),* **41**(3): 621-626.

Rosgen, D.L. 2001. The Cross-Vane, W-Veir and J-Hook Vane Structures: Their Description, Design and Application for Stream Stabilization and River Restoration. *Proc., Wetland Engineering and River Restoration Conf.(CD-ROM), ASCE*, Reston, Va.

Schoklitsch, A. 1932. Kolkbildung unter uberfallstrahlen. *Wasserwirtschaft*, 343.

Scurlock, S.M., Thornton, C. I. and Abt S. R. 2011. One-Dimensional Modelong Techniques for Energy Dissipation in U-Weir Grade-Control Structures. *World Environmental and Water Resources Congress, ASCE*. 2496-2507.

Scurlock, S.M., Cox, A. L., Thornton, C. I. and Baird, D. C. 2012a. Maximum Velocity Effects from Vane-Dike Installations in Channel Bends. *World Environmental and Water Resources Congress*, *ASCE*. 2614-2626.

Scurlock, S.M., Thornton,C. I. and Abt S. R. 2012b. Equilibrium Scour Downstream of Three-dimensional Grade-control Structures. *J. Hydraul.Eng., ASCE*, **138**(2): 167-176.

Shields, F. D., JR, Knight, S. S. and Cooper, C. M. 1995. Incised Stream Physical habitat Restoration with Stone Weirs. *Regulated rivers: Research and Management*, **10**: 181-198.

Veronese, A. 1937. Erosioni di fondo a valle di uno scarico. *Annali. dei Lavori Pubblci*., 75(9): 717–726 (in Italian).

Whittaker, W., and Jaggi, M. 1996. Blockshwellen. *Mitteilungen 91, Versuchsanstalt fur Wasserbrau, Hydrologie und Glaziologie*, ETH, Zurich, Switzerland.

Table 1, the characteristics of the tested wood structures.

l (m)	h_{st} (m)	α
0.533	0.085 , 0.055	30°
0.308	0.040 , 0.075	60°
0.267	0.041 , 0.062 , 0.081	90°

Table 2, Experimental test range

Test No.	Q (m^3/s)	α °	h_{st}(m)	l (m)	Δy (m)	h_{tw} (m)	z_m (m)
1	0.0040	90	0.041	0.267	0.0035	0.015	0.034
2	0.0070	90	0.041	0.267	0.0050	0.030	0.042
3	0.0100	90	0.041	0.267	0.0051	0.080	0.043
4	0.0150	90	0.041	0.267	0.0076	0.060	0.074
5	0.0250	90	0.041	0.267	0.0010	0.090	0.035
6	0.0350	90	0.041	0.267	0.0011	0.120	0.029
7	0.0450	90	0.041	0.267	0.0010	0.160	0.043
8	0.0550	90	0.041	0.267	0.0013	0.160	0.049
9	0.0150	90	0.062	0.267	0.0050	0.060	0.073
10	0.0200	90	0.062	0.267	0.0030	0.080	0.060
11	0.0250	90	0.062	0.267	0.0020	0.100	0.068
12	0.0350	90	0.062	0.267	0.0031	0.120	0.082
13	0.0550	90	0.062	0.267	0.0014	0.160	0.089
14	0.0100	90	0.081	0.267	0.0070	0.030	0.068
15	0.0150	90	0.081	0.267	0.0060	0.060	0.080
16	0.0250	90	0.081	0.267	0.0060	0.100	0.095
17	0.0350	90	0.081	0.267	0.0026	0.130	0.112
18	0.0450	90	0.081	0.267	0.0035	0.160	0.083
19	0.0100	60	0.040	0.308	0.0070	0.030	0.066
20	0.0150	60	0.040	0.308	0.0068	0.050	0.073
21	0.0200	60	0.040	0.308	0.0044	0.080	0.046
22	0.0300	60	0.040	0.308	0.0020	0.110	0.051
23	0.0400	60	0.040	0.308	0.0020	0.120	0.057
24	0.0500	60	0.040	0.308	0.0012	0.160	0.050
25	0.0100	60	0.075	0.308	0.0077	0.030	0.067
26	0.0200	60	0.075	0.308	0.0100	0.080	0.093
27	0.0250	60	0.075	0.308	0.0119	0.100	0.106
28	0.0450	60	0.075	0.308	0.0025	0.160	0.069
29	0.0100	30	0.055	0.533	0.0080	0.030	0.050
30	0.0150	30	0.055	0.533	0.0060	0.060	0.063
31	0.0200	30	0.055	0.533	0.0054	0.080	0.053
32	0.0300	30	0.055	0.533	0.0049	0.100	0.063
33	0.0400	30	0.055	0.533	0.0015	0.140	0.046
34	0.0500	30	0.055	0.533	0.0020	0.160	0.042
35	0.0100	30	0.085	0.533	0.0082	0.030	0.062
36	0.0250	30	0.085	0.533	0.0075	0.090	0.086
37	0.0300	30	0.085	0.533	0.0060	0.110	0.089
38	0.0350	30	0.085	0.533	0.0028	0.120	0.056
39	0.0400	30	0.085	0.533	0.0074	0.130	0.096
40	0.0450	30	0.085	0.533	0.0004	0.140	0.042

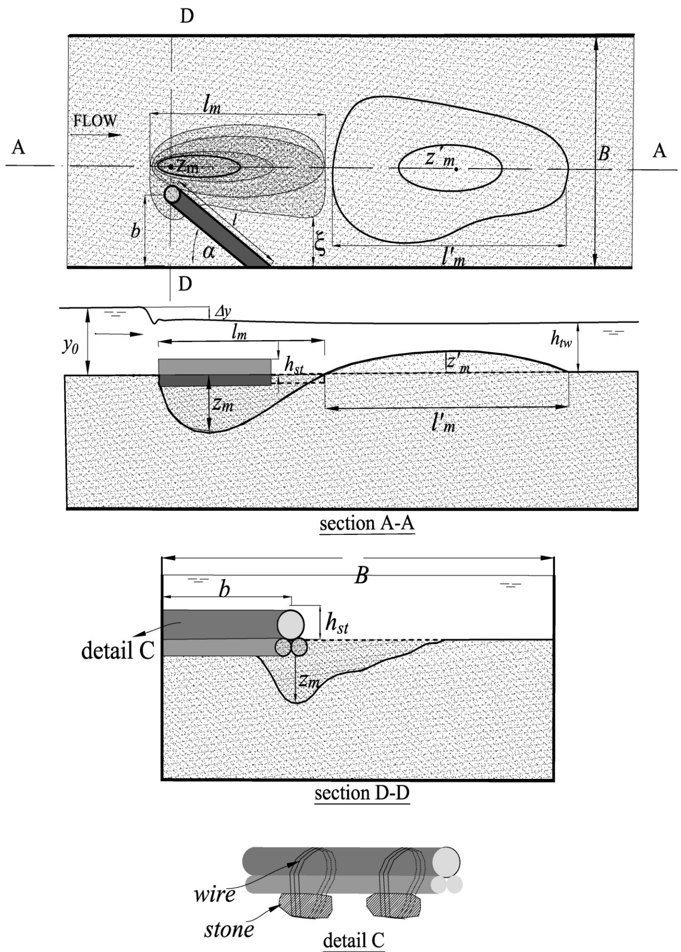

Fig.1 Plan, stream wise view A-A, cross section D-D with the main scour and flow parameters and the structure details (detail C).

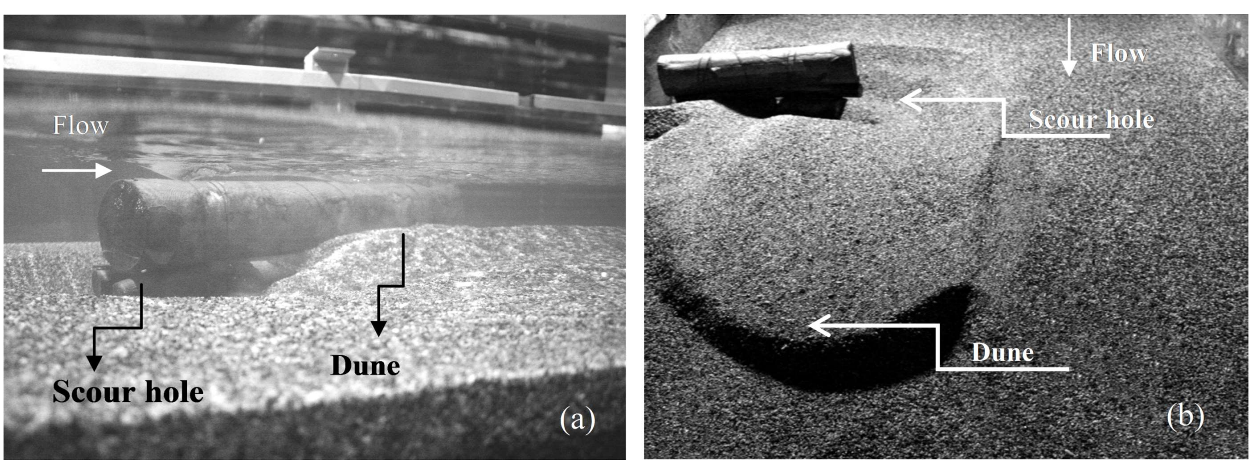

Fig. 2 a) View from upstream during a test run and b) View from downstream at the end of an experiment.

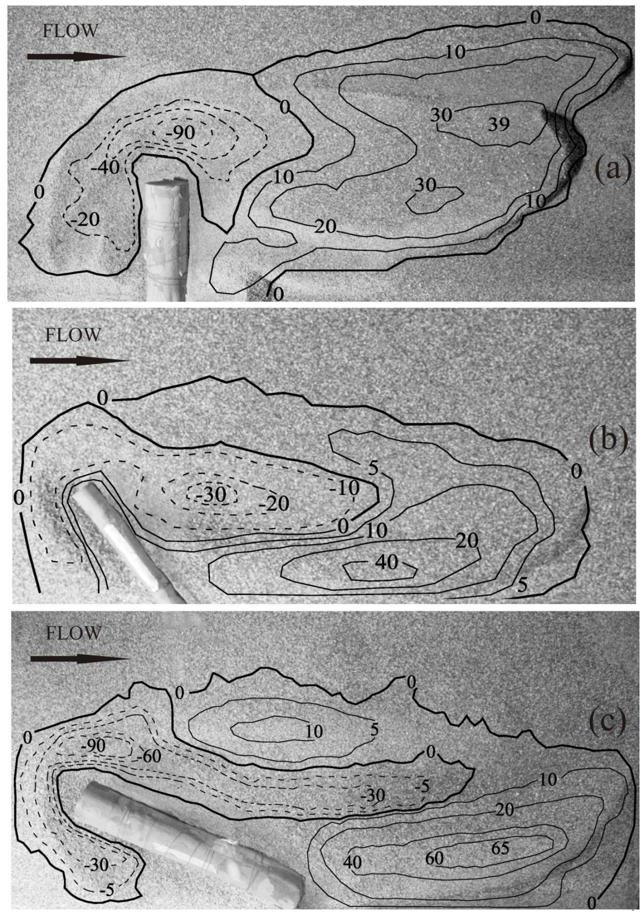

Fig. 3 Morphology of scour in Log-vane structure a) α=90°, Fd = 1.92, $\Delta y/h_{st}$ = 0.15, b) α=60°, Fd = 8.54, $\Delta y/h_{st}$ =0.03, c) α=30°, Fd = 1.86, $\Delta y/h_{st}$ = 0.09, on horizontal channel bed. The reference bed level is represented by the 0 mm contour line.

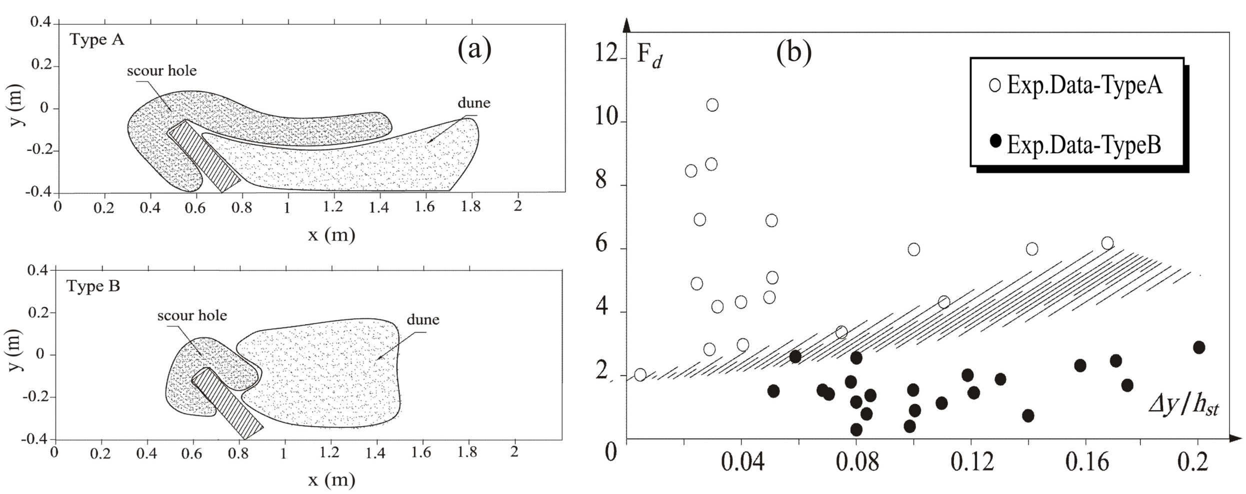

Fig. 4 a) Type A and Type B scour morphology b) Scour typology

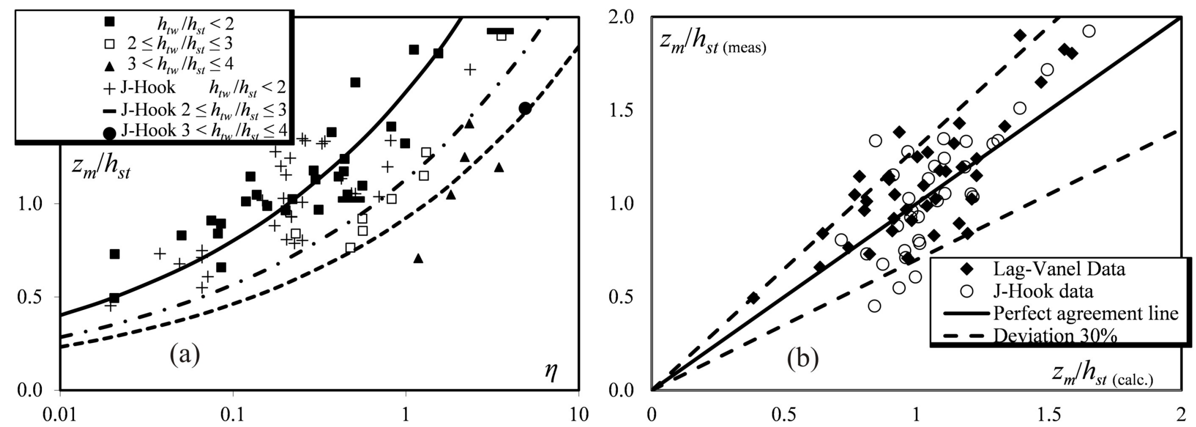

Fig. 5 a) Comparison of Eq. (3) with observed data and J-Hook data; [———] eq. (3) for h_{tw}/h_{st} = 1, [−· −· −] eq. (3) for h_{tw}/h_{st} = 2.5 and [---------] eq. (3) for h_{tw}/h_{st} = 3.5 b) Observed versus calculated scour depths z_m/h_{st} including J-Hook data

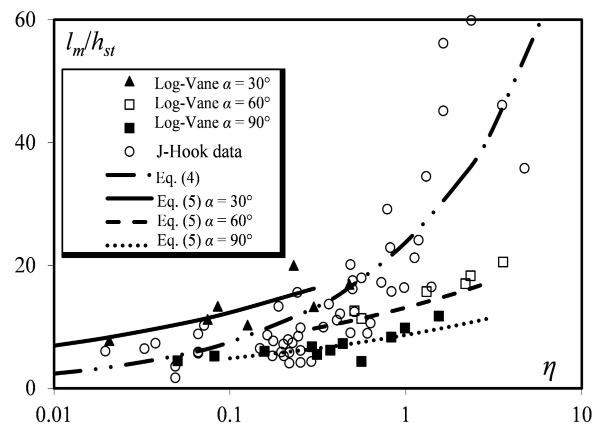

Fig. 6 Comparison Eq. (4) with observed data and J-Hook data

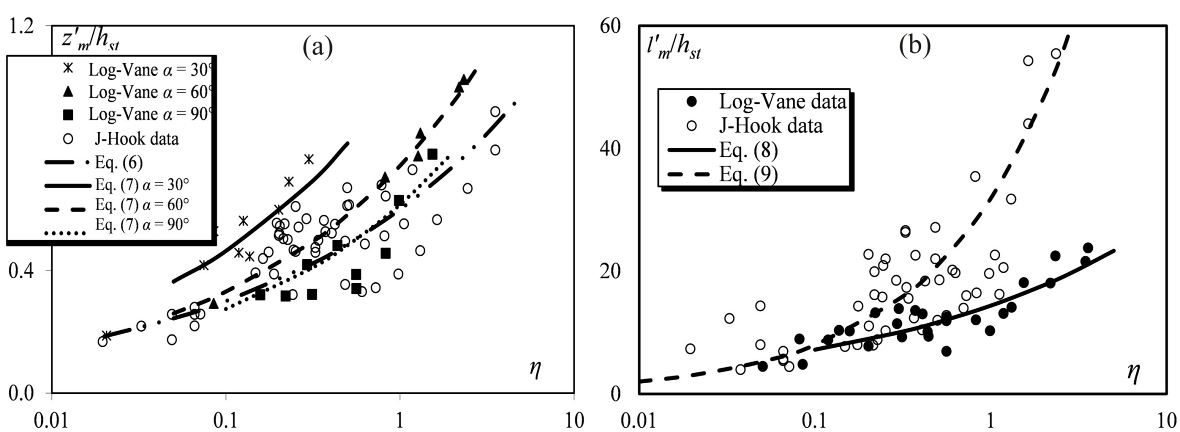

Fig. 7 a) Comparison eq. (6) and eq. (7) with observed data and J-Hook data b) Comparison between eq. (8) and eq. (9) with present and J-Hook data

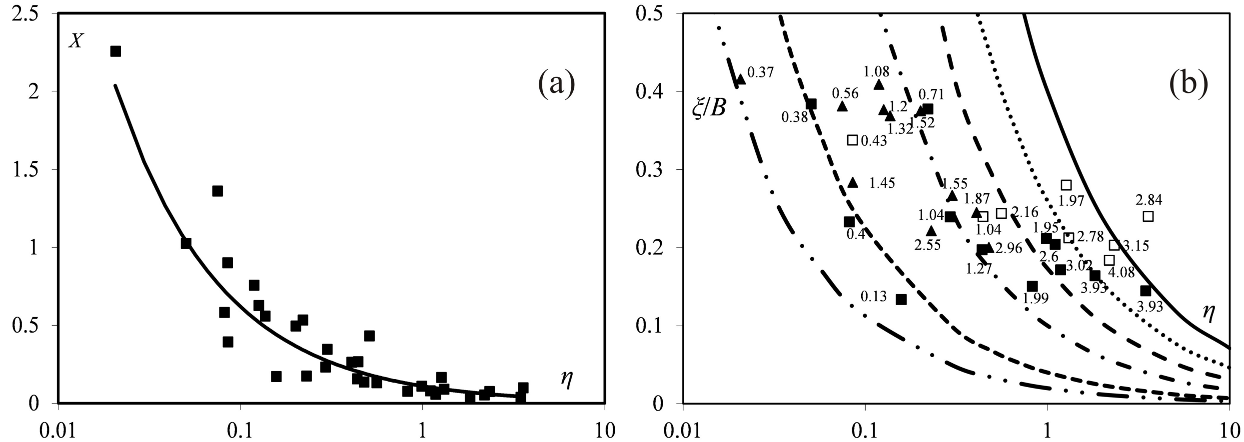

Fig. 8 a) Comparision of eq. (10) with the normalized parameter X . b) Comparison of Eq. (11) for different values of α and htw/hst with observed data; [‒••‒••‒] α = 30° & htw/hst = 0.4, [---------] α = 90° & htw/hst = 0.4, [———] α = 90° & htw/hst = 4, [‒• ‒• ‒] α = 90° & htw/hst = 1 and [•••••••] α = 60° & htw/hst = 3.